

## Bactericidal functionalization of wrinkle-free fabrics via covalently bonding TiO<sub>2</sub>@Ag nanoconjugates

C. Yang · G. L. Liang · K. M. Xu · P. Gao ·  
B. Xu

Received: 18 August 2008 / Accepted: 5 January 2009 / Published online: 11 February 2009  
© Springer Science+Business Media, LLC 2009

**Abstract** A simple technique is first developed to functionalize the durable-press all-cotton fabrics by grafting silver anchored TiO<sub>2</sub> (P25) nanoconjugates through enediol ligand-metal oxide bonding and resin dehydration. The functionalization is incorporated into a conventional pad-dry-cure process. The treatment ensures the nanoconjugates are covalently bonded to the substrate fabric materials (cotton cellulose). We tested the bactericidal activity of these surface-modified fabric samples after repeated laundries, using the waterborne *Escherichia coli* bacteria. Strong inhibition results were observed on the TiO<sub>2</sub>@Ag treated samples than using bare TiO<sub>2</sub> alone. After 60 min of sunlight irradiation, the overall bactericidal efficiency reached 96% after 7.5 h culturing. After 60 min of artificial solar light irradiation, the overall bactericidal efficiency reached 99%. Our observations suggest that the enediol linkage can be an effective candidate to graft functional metal oxide nanoconjugates onto a variety of fabric surfaces via a conventional pad-dry-cure process.

### Introduction

Because of the ever-growing demand for healthy and stylish living, there is a keen interest in natural fabric

garments capable of multiple functions, e.g., wrinkle resistance, good mechanical properties, anti-bacterial properties, sweat-absorbance, self-cleaning, etc. [1]. For example, durable-press treatment process has been applied to all-cotton textiles over decades. This treatment can provide wrinkle-resistant property to the textiles even after repeated laundries. There are many other reports on the functionalization of pure cotton textiles, e.g., sol-gel coatings or in situ polymerizations, which may provide such as the bactericidal property and water management property etc. [1–14]. In order to improve the durability of the capping materials, the exploration in the chemical bond between the capping materials and textile substrate is especially significant [15]. Therefore, developing methods that can induce covalent bonding of nanomaterials to textile surfaces with improvement of these drawbacks can be an interesting topic.

Selective bonding between photovoltaic materials and natural cellulose fabrics via chemical bond may be a powerful candidate to meet the above-mentioned requirements. For example, anatase phase TiO<sub>2</sub> is an efficient, non-toxic semiconductor photocatalyst that is widely used in the remediation of waste water and air pollution. Recently, efforts have been made to employ TiO<sub>2</sub> on fabrics in textile industry to utilize the redox properties of the catalyst as well as its antimicrobial properties [16–19]. For example, TiO<sub>2</sub> was coated onto cotton fabrics via an in situ low-temperature hydrothermal method [20]. There is also report about the surface modification of fabric surfaces using pre-hydrolyzed organically modified alkoxysilane (sol) filled with TiO<sub>2</sub> nanoparticles [1, 4]. Yet how to minimize the leaching effects and increase the photo-catalytic activity remains an aspect that needs to be addressed before these kinds of product become commercialized. In addition, the sol-gel method usually leads to

---

C. Yang · G. L. Liang · B. Xu  
Department of Chemistry, The Hong Kong University of Science and Technology, Clear Water Bay, Hong Kong, China

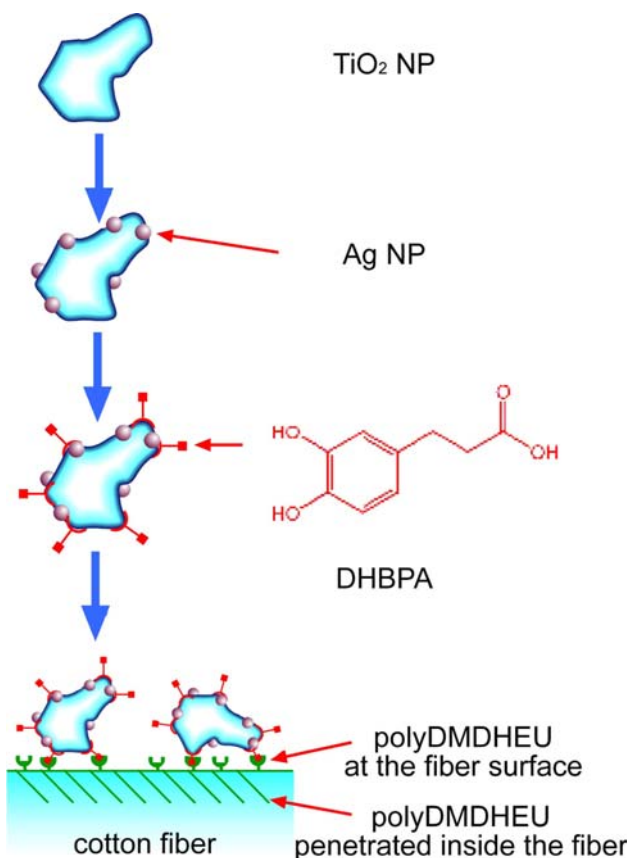
K. M. Xu · P. Gao (✉)  
Department of Chemical Engineering, The Hong Kong University of Science and Technology, Clear Water Bay, Hong Kong, China  
e-mail: kepgao@ust.hk

lower crystallinity of  $\text{TiO}_2$  due to the restricted curing time and temperature. On the other hand, as a necessity for the sol–gel reaction, prolonged curing time may impose an adverse effect on the mechanical properties of the textiles. Currently, only few reports on chemical bonding linkage have been reported which show reliability over repeated launderings [15].

When  $\text{TiO}_2$  is irradiated photons of equal or higher than its band gap energy, the electron-hole pairs generated by photoexcitation migrate to the  $\text{TiO}_2$  surface; the holes will oxidize the surface-adsorbed  $\text{H}_2\text{O}$  to produce the highly reactive hydroxyl radicals, which show strong oxidizing activity [21–24]. Intensive research work has been carried out in the past decade to shift the band gap of  $\text{TiO}_2$  to the visible range so that sunlight can be an optional source for photoactivation [25–30]. Most notable progress has been shown in the noble metal- $\text{TiO}_2$  nanoconjugate systems. The noble metals play a mediating role in storing and shuttling photogenerated electrons from  $\text{TiO}_2$  to an acceptor in a photocatalytic process. For example, metal or metal ion doped  $\text{TiO}_2$  composites exhibit shift in the Fermi level to more negative potentials, which improves the energetics of the composite system and enhances the efficiency of interfacial charge-transfer process [31–34]. In addition, doping noble metal onto  $\text{TiO}_2$  catalyst also imparts improved functionality of the composite. Zhang et al. [35] reported that silver anchored P25 nanoconjugates can enhance the anti-bacterial property under UV light.

Rajh et al. studied the enediol ligand binding efficiency of  $\text{TiO}_2$  nanoparticles in improving the optical response in the visible spectral region. A series of enediol ligands were found bearing the potency to adjust the coordination geometry of the  $\text{TiO}_2$  surface and shift the onset of absorption toward the visible region of the spectrum, compared to unmodified nanocrystallites [36]. The dipole moment between the enediol and  $\text{TiO}_2$  has been simulated [36]. The enediol ligand bond was proven to be dependent on the coordination geometry of the surface Ti atoms, and only bind to parts of the surface area of the nanoparticles [36].

In this article, we present an effective method by applying the surface-functionalized  $\text{TiO}_2@Ag$  nanoconjugates on cotton textiles via a pad-dry-cure process, which is a conventional treatment process to impose durable press wrinkle-resistant property to the textiles. As shown in Scheme 1, the surface of the  $\text{TiO}_2@Ag$  nanoconjugates was pre-modified by using 3-(3,4-dihydroxyphenyl)propionic acid (DHBPA) [34], which bears carboxylic acid groups (i.e. reactive to the resin crosslinkers and cellulose substrate). During the curing step in a durable press process, the pending carboxylic acid group can react with the hydroxyl groups on dimethyloldihydroxyethyleneurea (DMDHEU) (via ester bond) to anchor the nanoconjugates



**Scheme 1** Schematic illustration of the formation of  $\text{TiO}_2@Ag$  nanoconjugate, its functionalization, and grafting onto cotton fabric surface. PolyDMDHEU is the resin for durable press treatment

to the surface of the cotton fabric sample. While for the bare  $\text{TiO}_2$  surface, DMDHEU does not link to it. Durability of such treatment will be demonstrated through repeated laundries of up to 25 washes. The bactericidal activity of these fabric samples after 5 washes was assayed using the Gram-negative bacteria *E. coli*, under sunlight at ambient temperature. The  $\text{TiO}_2@Ag$  nanoconjugates grafted fabric samples showed a much stronger inhibition effect to the bacteria than  $\text{TiO}_2$  nanoparticles (P25) grafted fabric samples as well as the bare fabric samples. The fabric samples after prolonged washing up to 25 times were evaluated under artificial sunlight (metal halide lamp). Enhanced bactericidal effect was observed compared to P25 treated sample.

## Experimental procedures

### Materials

P25 (Degussa), 3-(3,4-dihydroxyphenyl)propionic acid (DHBPA) (Aldrich, 99%), silver nitrate (Aldrich, 99%), dimethyloldihydroxyethyleneurea (DMDHEU) (FREEREZ<sup>®</sup>)

980, Novenon Inc.), ammonium hydroxide (Fisher, 30%), magnesium chloride hexahydrate (Fluka, 99%), Triton X-405 (IL, 75% solution) were used without further purification. Deionized (DI) water was purified with Milli-Q system (Millipore, >18 mΩ). *E. coli* was from ATCC. The fabric samples had the dimension of 15 × 15 in. and were all pure cotton.

#### Synthesis of silver anchored TiO<sub>2</sub>

The method for anchoring silver onto TiO<sub>2</sub> nanoparticles is similar to the work developed by Zhang et al. [35]. TiO<sub>2</sub> powder (1.00 g) (P25, Degussa) was suspended in 40 mL ethanol solution with 0.10 v/v% Triton X-405, followed by addition of an appropriate amount of 0.1 M [Ag(NH<sub>4</sub>)<sub>2</sub>]<sup>+</sup> aqueous solution [35]. Two conditions were used: one is 0.25 mL of [Ag(NH<sub>4</sub>)<sub>2</sub>]<sup>+</sup> solution and the other is 0.5 mL [Ag(NH<sub>4</sub>)<sub>2</sub>]<sup>+</sup> solution. The suspension was then stirred for 5 h for reaction. During stirring, the color of the suspension gradually changed from white to purple. The purple powder was recovered by centrifugation and washing. Finally it was totally dried under vacuum at 60 °C for 8 h.

#### Characterization of TiO<sub>2</sub>@Ag nanoconjugates

UV–Visible absorption spectra of colloidal solutions were recorded by a Perkin-Elmer double beam scanning spectrometer, model Lambda 20. Each sample was centrifuged at 5000 rpm and washed three times. The precipitates were dispersed into 1 mM aqueous suspension. FT-IR experiments were performed on a Perkin-Elmer Spectrum One Fourier transform infrared spectrometer. All samples were prepared by mixing with KBr prior to testing. Sixteen scans were performed for each spectrum. The morphology and size of the nanoconjugates were studied on a JEOL 2010F transmission electron microscope (TEM) operating at 200 keV and 96 μAm, equipped with a Gatan CCD camera and an OXFORD Inca EnergyTEM200 electron dissipation spectroscopy (EDS) system. X-ray photoelectron spectroscopy (XPS) measurement was performed on a Physical Electronics PHI 5600. Scanning electron microscope (SEM) images of the nanoconjugate treated fabric were obtained: Small pieces of textile samples after washing for five times were stuck on a Torr-Seal epoxy (Varian) and sputtered with 12.5 nm of gold. The resulting samples were imaged using a JEOL 6700F microscope.

#### Surface functionalization of TiO<sub>2</sub>@Ag nanoconjugates using DHBPA

A total of 1.00 g of bare TiO<sub>2</sub> (P25), nanoconjugate sample 1 (AT025), nanoconjugate sample 2 (AT050) was dispersed into 100 mL aqueous solution of 10 mg DHBPA,

respectively. The mixture was stirred for 5 min at room temperature, and the solids were centrifuged at 500 rpm for 5 min and washed two times. Product was collected and labeled with the concentration.

#### Cotton fabric treatment (nanoconjugates and resin)

Fabric samples were all treated using the TiO<sub>2</sub>@Ag nanoconjugates according to the following method.

In total, 150 mL DMDHEU, 12.0 g MgCl<sub>2</sub>, and 5.0 g of dry nanoconjugate powder were mixed together into 750 mL aqueous suspension in DI water. It was mechanically stirred for 1 min before each component was well-mixed. A piece of textile sample with the dimension of 15 × 15 in. was dipped in the bath of the suspension, and then washed gently for 7 min. Then, the textile sample was picked up and padded at a pressure of 15 kg/cm<sup>2</sup> with a 78% wet-pickup. Afterwards, it was placed into a 3-kg tumble dryer (ZANUSSI TD-892N) and dried at 60 °C to achieve 25 wt% wet-pickup. Then, the sample was hand ironed at 110 °C to remove wrinkles before it was cured at 135 °C for 10 min in a Memmert ULE500 oven. (This treatment process achieves grade 4.5 of durable-press rating (5 grades.) (AATCC Test Method 124-1969) [37, 38].

#### Washing the fabric samples

The washing method to the fabric samples follows AATCC Test Method 124-1969 [37, 38].

#### Determination of bactericidal property of the nanoconjugate treated textiles on *E. coli* under dark condition

The bactericidal property of the treated fabrics was tested on *E. coli* under dark condition. The bacteria were cultivated in 5 mL NB broth (containing 10 g/L peptone, 10 g/L beef extract, 5 g/L sodium chloride). The bacterial cell concentration was measured using the optical density at 600 nm and the cell number was calculated based on the standard calibration (with the assumption that an optical density of 1.0 at 600 nm is equivalent to approximately 10<sup>8</sup> cells per mL). Waterborne bactericidal assay was carried out as follows.

The bacterial suspension of concentration of 10<sup>5</sup>/mL was prepared. Sterilized fabric samples with dimensions of 1 × 1 cm were immersed in the above suspension in a sterile flask. The flask was then shaken at 200 rpm at 37 °C for 24 h. The fabric sample was then taken out, washed, and prepared for characterization by SEM. The residue broth was also tested using the optical density measurement, and the actual bacterium number within the broth was calculated. The sample fixation and preparation

process for SEM was as follows: the substrates were first washed with PBS immediately after the incubation period, and 3 v/v% glutaraldehyde in PBS was added for fixation and stored at 4 °C for 5 h. After the glutaraldehyde solution was removed, the substrates were washed with PBS, followed by step dehydration with 25, 50, 70, 95, and 100% (by volume) ethanol for 10 min each. The substrates were then dried and sputter-coated by gold. The SEM characterization was carried out on a JEOL 6700F SEM.

Determination of light-irradiated bactericidal property of the nanoconjugates treated textiles on *E. coli*

In this test, we measured the bactericidal property (based on *E. coli*) of the nanoparticles (including pure P25 and silver anchored P25 nanoconjugates) under direct sunlight irradiation and under metal halide lamp irradiations.

The bacteria were cultivated in 5 mL of NB broth. The bacterial cell concentration was measured using optical density at 600 nm, and the cell number was calculated based on the standard calibration with the assumption that an optical density of 1.0 at 600 nm is equivalent to approximately  $10^8$  cells per mL. Waterborne bactericidal assay was carried out as follows.

The bacterial suspension of concentration of  $10^5$  mL<sup>-1</sup> was prepared. The sterilized fabric samples with the dimension of 1 × 1 cm were soaked with 0.2 mL suspension in a sterile flask. The flask was then shaken at 200 rpm at 37 °C for 3 h. The fabric sample was then taken out, washed with DDI water, and irradiated under direct sunlight (1.25 mW/cm<sup>2</sup> or UV index 5) for 60 min in 2 mL DDI water, then cultured for 9 h in broth. The fabric samples were washed and prepared for characterization by SEM. The residue broth was also tested by optical density measurement, and the actual bacterium number within the broth was calculated. The sample fixation and preparation for SEM were the same as mentioned in the previous section.

In order to evaluate the long-term reliability of the bactericidal effect of this fabric surface modification, we also tested the bactericidal property of the nanoconjugates treated textiles on *E. coli* under metal halide lamp irradiation (high-intensity discharged arc light source) [39]. Before this examination, all fabric samples were washed for 25 times to examine the long-term reliability. The light source (JLZ-70W) can provide a full spectrum white light, with the unit energy output similar to the natural sunlight when the bacterium samples were placed 15 cm (1.0 mW/cm<sup>2</sup>) to the light source (central ~100 mW/cm<sup>2</sup>), which is operating at its designed full power. The rest of the sample treatment processes were the same to the prior test which was under sunlight.

## Results and discussion

### Optical properties and morphology of the nanoconjugates

The silver anchored TiO<sub>2</sub> nanoconjugates show different colors in the photographic image (Fig. 1). When DHBPA was applied on the P25 nanoparticles, the bright white color of the nanoparticle suspension turned into pale yellow, which showed the surface grafting of the molecule. The shift of UV–Vis absorption wavelength is due to the anchoring of silver nanoparticles onto TiO<sub>2</sub> surface (Fig. 2). Figure 2 also shows that with the increase of silver content, the UV absorption increases and the peak position



**Fig. 1** Photographic image of surface modified P25 nanoparticles and the nanoconjugates of TiO<sub>2</sub>@Ag. (a) 5 g/L AT050 functionalized with DHBPA; (b) 5 g/L AT050; (c) 5 g/L AT025; (d) 5 g/L bare P25; and (e) 5 g/L bare P25 functionalized by using DHBPA

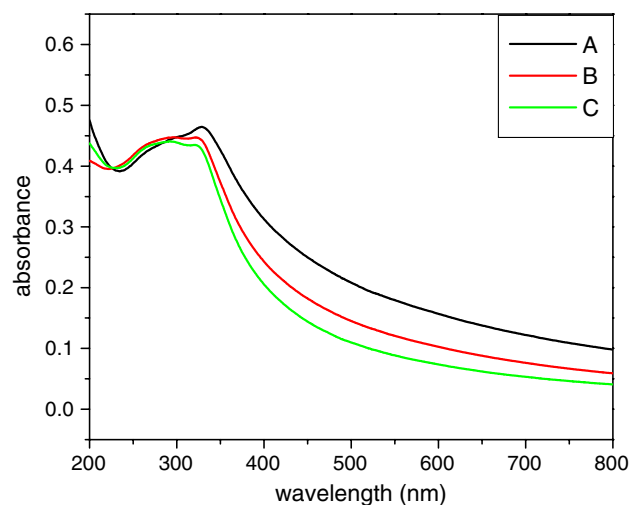


**Fig. 2** UV–Vis absorption of a 1 mM TiO<sub>2</sub>@Ag solutions with 0.1% Triton X-405. Concentrations of silver for each nanoconjugate sample are (a) 0.5 mmol/g TiO<sub>2</sub> (AT050), (b) 0.25 mmol/g TiO<sub>2</sub> (AT025), and (c) TiO<sub>2</sub> (P25)

shows clear red shift to the visible wavelength region. The intensity of the UV–Vis absorption in the visible region also increases, which was attributed to the UV absorption of silver [35].

#### Morphological analysis of TiO<sub>2</sub>@Ag nanoconjugates

Figure 3 shows both the overview of TEM image of silver functionalized TiO<sub>2</sub> nanoconjugate (sample AT025) and the HRTEM image of the silver-coated TiO<sub>2</sub> and the corresponding EDS spectra of the anchored silver nanoparticle and TiO<sub>2</sub> region. Since the concentration of silver is very low, electron diffraction pattern (EDP) only shows the strong crystallinity of anatase phase TiO<sub>2</sub> of the nanoconjugate (Fig. 3a inset). (Powder X-ray diffraction analysis of the TiO<sub>2</sub>@Ag samples also showed negligible intensity of silver signals, which is not shown in this article.) When the reduction of [Ag(NH<sub>4</sub>)<sub>2</sub>]<sup>+</sup> takes place in situ on the TiO<sub>2</sub> particles, silver nanoparticles with the size around 5 nm form on TiO<sub>2</sub> with high dispersity. Under TEM, the silver nanoparticles are all in the size smaller than 8 nm. From TEM studies, no non-supported silver nanoparticles were found, which indicates that silver particles were strongly anchored to the TiO<sub>2</sub> supports. Triton X-405 and TiO<sub>2</sub> nanoparticles help prevent the aggregation of silver clusters. HRTEM images (Fig. 3b) indicate crystalline silver particle is in close contact with the TiO<sub>2</sub> support. This close contact is believed to favor the electron transfer between silver and TiO<sub>2</sub> [40]. XPS analysis on the as-prepared nanoconjugates is presented in Fig. 4 and Table 1, which show the successful anchoring of silvers on the TiO<sub>2</sub> nanoparticles.

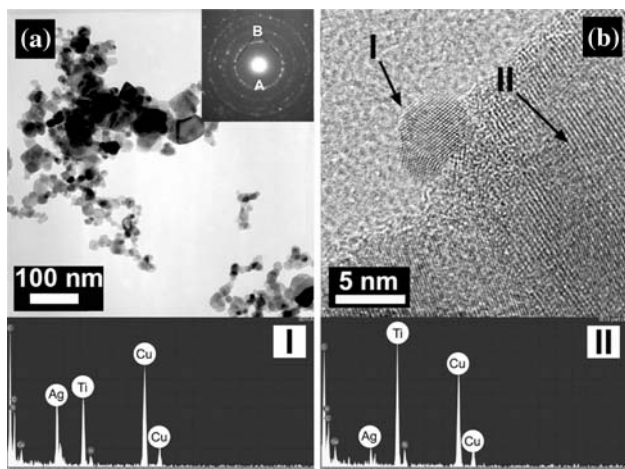


**Fig. 3** **a** TEM overview image of TiO<sub>2</sub>@Ag nanoconjugates (AT050), the inset EDP pattern shows the diffraction of TiO<sub>2</sub>. Ring A refers to the D-spacing 3.56 Å, ring B refers to the D-spacing 3.26 Å. **b** HRTEM of TiO<sub>2</sub>@Ag nanoconjugates (AT050) and EDAX spectra showing (I) the existence of silver and (II) TiO<sub>2</sub> corresponding to the HRTEM image

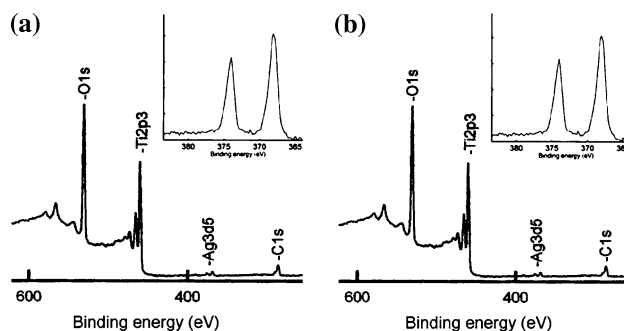


**Fig. 4** XPS analysis of TiO<sub>2</sub>@Ag nanoconjugates **a** AT025 and **b** AT050 (inset shows the corresponding magnified spectra indicating silver)

**Table 1** TiO<sub>2</sub> to silver ratio and yields of the two nanocomposites (AT025 and AT050)

	Atomic concentration		Silver content (%)
	Ti	Ag	
AT025	25.99	0.17	0.65
AT050	26.33	0.38	1.42

#### Surface structure of DHBPA functionalized nanoconjugates

When TiO<sub>2</sub> particles are in nanocrystalline regime, a large fraction of the atoms located at the surface may have significantly altered electrochemical properties, especially for the atoms at the corner or at the edge of the nanoparticles. Concerning their weaker covalent bonding with solvent species compared to those bonding within the lattice, the energy level of the surface species is decreased with their redox abilities [36, 41]. The size effect of the nanocrystalline also adjusts the Ti atoms coordination type from hexacoordinated (octahedral) to pentacoordinated (square pyramidal) [41]. This enhances the binding between enediol ligands and Ti atoms on TiO<sub>2</sub> nanoparticles with even larger sizes. As a result, the surface capped TiO<sub>2</sub> nanoparticles and TiO<sub>2</sub>@Ag nanoconjugates show red-shift absorption, as can be seen in Fig. 1. Since P25 has an irregular geometry, it remains a large area of TiO<sub>2</sub> surface unreacted even after resin treatment. Figure 5a shows the IR absorption of the solid samples of P25, nanoconjugates (AT025), DHBPA treated pure P25 and DHBPA (after repeated washes and dried). Bidentate binding between the nanoconjugates and DHBPA was confirmed by FT-IR spectra. For example, the aryl oxygen stretching at 1250 cm<sup>-1</sup> was not affected by DHBPA adsorption at the surface of P25 (Fig. 5(I)). This bidentate binding with ortho hydroxyl groups of enediol ligands suggests the formation of a five-membered ring around the surface Ti atoms, which is a favorable conformation of bond angles

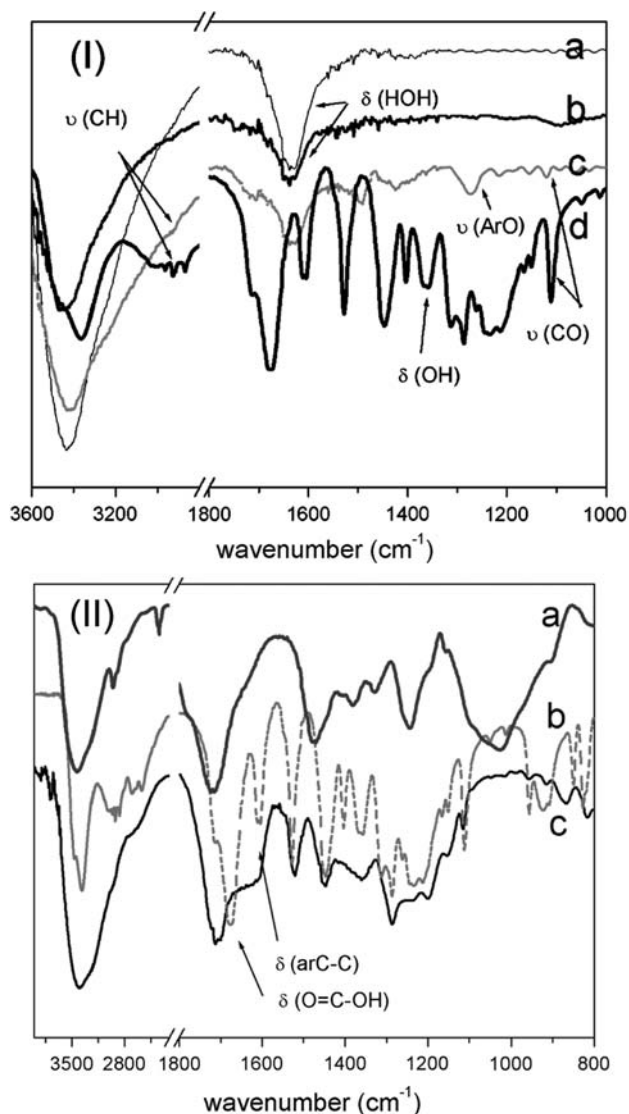


**Fig. 5** (I) FT-IR absorbance of TiO<sub>2</sub>@Ag nanoconjugates. (a) Dried TiO<sub>2</sub>@Ag nanoconjugate AT025, (b) dry bare TiO<sub>2</sub> (P25), (c) 100 mg/L DHBPA modified 10 g/L TiO<sub>2</sub> (P25) at pH 3 dried thoroughly in ethanol, and (d) DHBPA. (II) FT-IR absorbance of (a) DHBPA, (b) DMDHEU after curing at 140 °C for 1 h, and (c) 1:1 DMDHEU to DHBPA after curing at 140 °C for 1 h

and distances for the octahedral coordination of the surface Ti atoms. We can also observe that the bending vibrations of phenyl OH groups at 1365 cm<sup>-1</sup> disappear while the CH groups of benzene ring retain, and observed the vibrations of the aryl CH groups (3050 cm<sup>-1</sup>) as well as the aryl oxygen stretching at 1250 cm<sup>-1</sup>. In Fig. 5(II-c), no peak can be found at 1680 cm<sup>-1</sup>, which suggests no C=O vibration of carboxylic acid of DHBPA; however, to compare with the crosslinked DMDHEU (a), the peak denoting the vibration of C=O bond gets broader, which shows the formation of a new ester bond between the acid and the hydroxyl groups from DMDHEU. We can also observe that for (c), the peak at ~1600 cm<sup>-1</sup> (the

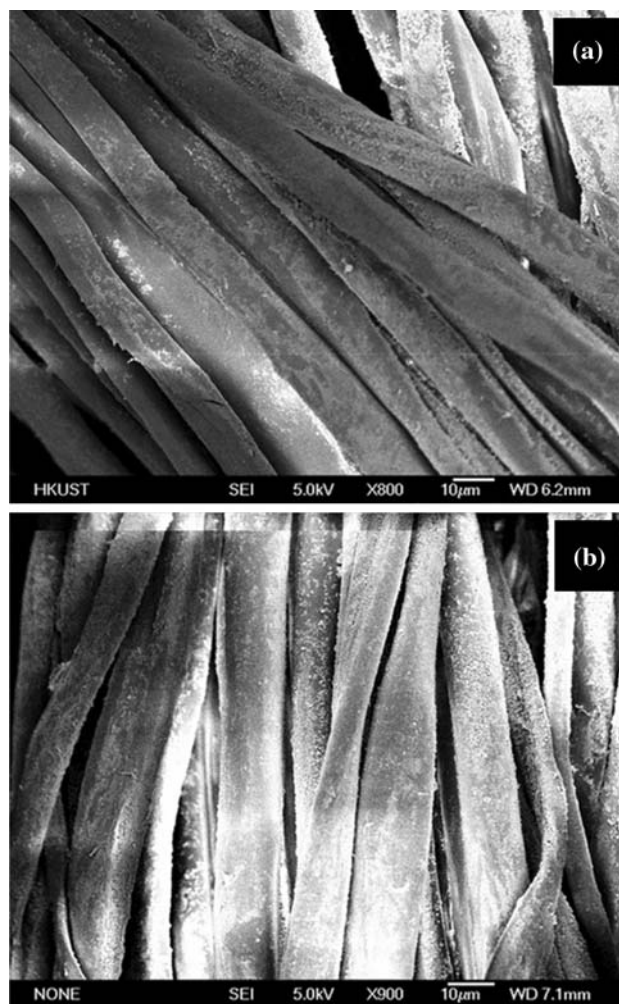


**Fig. 6** SEM of **a** TiO<sub>2</sub>@Ag nanocomposite (AT050) treated fabric and **b** TiO<sub>2</sub>@Ag nanocomposite (AT050) treated fabric after 25 washes

stretching vibration of aryl carbons) is broader than DHBPA (b), which indicates the phenol group on the freestanding DHBPA has reacted with DMDHEU. From the SEM images (Fig. 6) we can see that after 25 laundries, there is still a layer of functionalized AT050 nanoconjugates on the cotton surface, while using bare AT050, after laundries, we did not observe any nanoconjugate at the surface. This result also confirms the IR data which show a covalent bond between the nanoconjugates with DHBPA, which therefore has the higher reactivity to resin.

#### Bactericidal activity analysis of the nanoconjugates treated textiles

It has been well documented that a small amount of silver does not cause harmful health problems, but it will provide an efficient bactericidal function. TiO<sub>2</sub> is also an efficient candidate which shows a certain bactericidal property

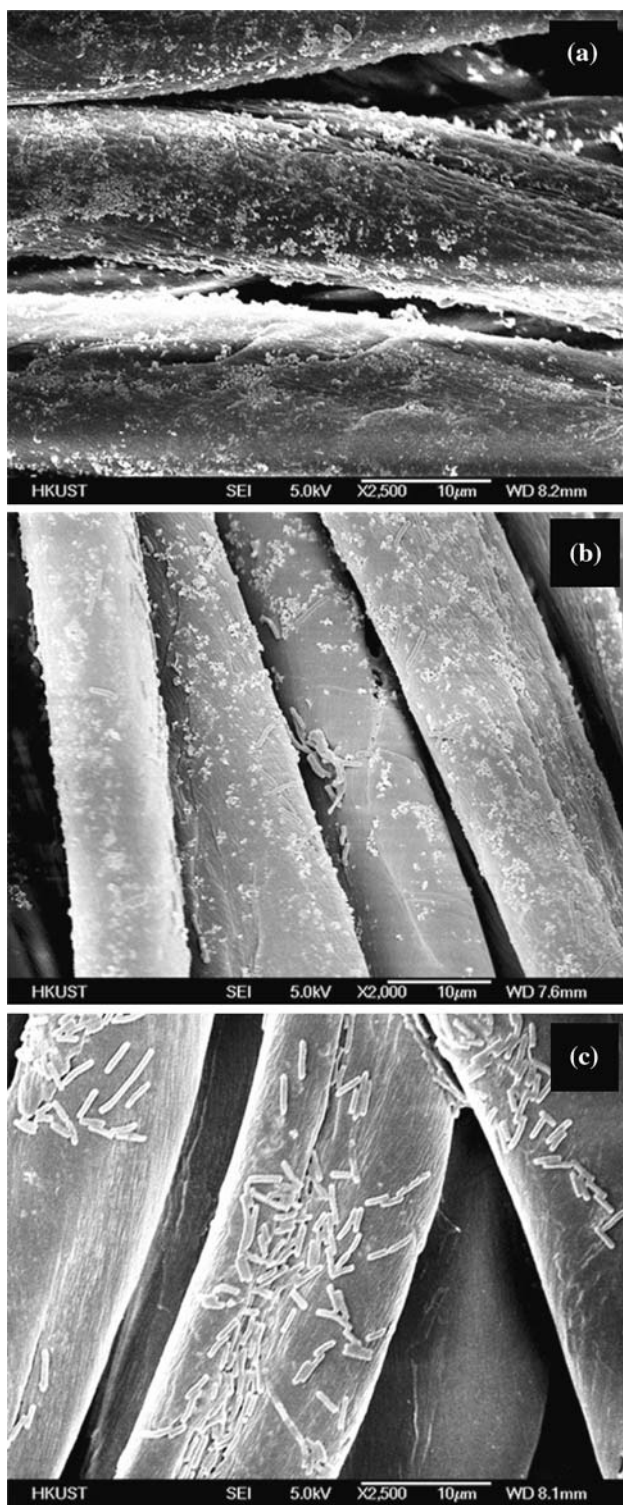


**Fig. 7** SEM images of DMDHEU treated fabric (for each after five washes) after waterborne bacteria (*E. coli*) assay, which include **a** fabric with  $\text{TiO}_2@Ag$  (AT050), exposed to sunlight for 30 min, **b** fabric with  $\text{TiO}_2$  (P25), exposed to sunlight for 30 min, and **c** fabric only treated with DMDHEU, exposed to sunlight for 30 min

under UV light [42]. The nanoconjugate (AT050) and bare  $\text{TiO}_2$  (P25) treated wrinkle-free fabric sample were assayed the bactericidal property (*E. coli*) in aqueous solution. The wrinkle-free cotton fabric samples without surface grafting were used as the control. In our experiment, no cell damage was observed after they were cultured in normal broth with the existence of pure cotton textiles. Figure 7a shows the fabric samples with the surface grafted with  $\text{TiO}_2@Ag$  nanocomposite (through DHBPA) by a conventional pad-dry-cure process, and Fig. 7b shows the sample treated (through DHBPA) with bare  $\text{TiO}_2$  (P25) using the same pad-dry-cure processing protocol. Figure 7c shows the fabric sample without surface grafting. Numerous bacteria in the interstitial spaces and along the fibers of the fabric sample are observed in Fig. 7c. The test was carried out at ambient temperature (23 °C) and exposed to direct sunlight (1.25 mW/cm<sup>2</sup> or UV index 5). The PBS solution with the *E. coli* contaminated fabric samples were irradiated for 60 min, respectively. Then, the fabric samples were transferred into broth and shaken for 7.5 h. The resulting cell counts were conducted following OD600. In Fig. 8, we can observe that both the light irradiation (including sunlight and artificial sunlight) inhibit the bacterial growth to a certain extent, compared to the dark environment. We can also observe that the P25 surface modification did not show a significant inhibition effect than the control bare sample, when the fabric samples were irradiated with sunlight/artificial sunlight for 60 min. However, the nanoconjugate (AT050) treated fabric showed an almost 100% inhibition to *E. coli* after the irradiation of both sunlight and artificial sunlight. This result shows that silver anchored  $\text{TiO}_2$

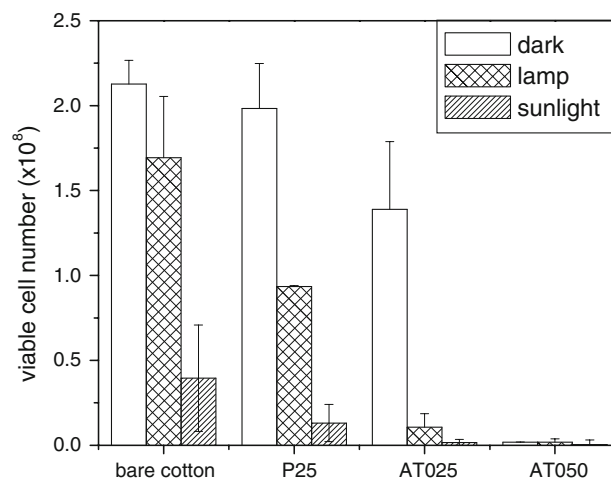


**Fig. 8** Bacterium counts in the remained broth (in dark/artificial sunlight (after 25 washes)/sunlight (after 5 washes) irradiation). The cell solutions were diluted by 10 times before counting

functionalizes as a strong inhibitor to *E. coli*; however, the bare P25 does not. For sample AT025 treated fabric, light-induced bactericidal effect is quite significant; while for sample AT050, it contains higher amount of silver, so the silver effect is predominant. Both AT025 and AT050 treatments showed more efficient bactericidal effect toward the fabric sample than P25 treatment. This result shows that silver functionalizes as a strong inhibitor to *E. coli*; however, the bare P25 appears to show a weak bacterial inhibition effect when irradiated using direct sunlight or artificial sunlight.

## Conclusion

In this study, an innovative method combining nanoconjugates covalently linking to the durable-press fabrics was developed for the enhancement of bactericidal property. By modifying the surface of silver anchored TiO<sub>2</sub> nanoconjugates using DHBPA through a specific chelation process, we have demonstrated that this kind of surface-modified nanoconjugates can act as a useful agent to provide the bactericidal property to the wrinkle-free all-cotton textiles in a facile and efficient way. This treatment effectively improves the bactericidal property of the wrinkle-free cotton textiles. Ene-diol bonding can efficiently graft TiO<sub>2</sub> nanocrystals onto cotton fabrics and the TiO<sub>2</sub> can improve the antibacterial property after laundries. Compared to the bare TiO<sub>2</sub> functionalized fabric samples, covalently bonding silver anchored TiO<sub>2</sub> nanoconjugates to the fabric surface can effectively inhibit *E. coli* under both sunlight and artificial sunlight. The treatment is resistant to repeat washes. It shows the potentials in overcoming the difficulties encountered by the ordinary methods, with its advantages of high-performance, easy-care, and low-processing requirements. This method is also suitable for other nanoconjugate systems which have a reduced surface with octahedral cell geometry to bond with catachol group, such as Fe<sub>3</sub>O<sub>4</sub> nanoconjugates or other metal oxides nanoconjugates [36, 43]. Further experiments to validate the efficiency of this treatment method with respect to improving the other functionalities of durable-press cotton textiles are valuable.

**Acknowledgement** This research was supported by ITF, grant no. UIM109 (The Hong Kong University of Science and Technology).

## References

- Mahltig B, Haufe H, Bottcher H (2005) *J Mater Chem* 15:4385
- Qi KH, Daoud WA, Xin JH, Mak CL, Tang WZ, Cheung WP (2006) *J Mater Chem* 16:4567
- Qi KH, Chen XQ, Liu YY, Xin JH, Mak CL, Daoud WA (2007) *J Mater Chem* 17:3504
- Tarimala S, Kothari N, Abidi N, Hequet E, Fralick J, Dai LL (2006) *J Appl Polym Sci* 101:2938
- Tiller JC, Liao CJ, Lewis K, Klibanov AM (2001) *Proc Natl Acad Sci USA* 98:5981
- Onar N, Sariisik M (2004) *J Appl Polym Sci* 93:2903
- Oktem T (2003) *Color Technol* 119:241
- Lee HY, Park HK, Lee YM, Kim K, Park SB (2007) *Chem Commun* 2959
- Klueh U, Wagner V, Kelly S, Johnson A, Bryers JD (2000) *J Biomed Mater Res* 53:621
- Kittinaovarat S, Kantuptim P, Singhaboonponp T (2006) *J Appl Polym Sci* 100:1372
- Hong KH, Sun G (2007) *J Appl Polym Sci* 106:2661
- Gao Y, Cranston R (2008) *Text Res J* 78:60
- El-Tahlawy KF, El-Bendary MA, Elhendawy AG, Hudson SM (2005) *Carbohydr Polym* 60:421
- Cen L, Neoh KG, Kang ET (2004) *J Biomed Mater Res A* 71A:70
- Fir M, Vince J, Vuk AS, Vilcnik A, Jovanovski V, Mali G, Orel B, Simoncic B (2007) *Acta Chim Slov* 54:144
- Wang CC, Chen CC (2005) *Appl Catal A Gen* 293:171
- Sunada K, Kikuchi Y, Hashimoto K, Fujishima A (1998) *Environ Sci Technol* 32:726
- Maness PC, Smolinski S, Blake DM, Huang Z, Wolfrum EJ, Jacoby WA (1999) *Appl Environ Microbiol* 65:4094
- Amezaga-Madrid P, Silveyra-Morales R, Cordoba-Fierro L, Nevarez-Moorillon GV, Miki-Yoshida M, Orrantia-Borunda E, Solis FJ (2003) *J Photochem Photobiol B* 70:45
- Daoud WA, Xin JH (2004) *J Am Ceram Soc* 87:953
- de Oliveira AL, Wolf A, Schuth F (2001) *Catal Lett* 73:157
- Linsebigler AL, Lu GQ, Yates JT (1995) *Chem Rev* 95:735
- Kamat PV (1993) *Chem Rev* 93:267
- Rolison DR (2003) *Science* 299:1698
- Jakob M, Levanon H, Kamat PV (2003) *Nano Lett* 3:353
- Cozzoli PD, Fanizza E, Comparelli R, Curri ML, Agostiano A, Laub D (2004) *J Phys Chem B* 108:9623
- Hirakawa T, Kamat PV (2005) *J Am Chem Soc* 127:3928
- Yang ZX, Wu RQ, Goodman DW (2000) *Phys Rev B* 61:14066
- Valden M, Lai X, Goodman DW (1998) *Science* 281:1647
- Sun B, Vorontsov AV, Smirniotis PG (2003) *Langmuir* 19:3151
- Tada H, Teranishi K, Inubushi Y, Ito S (1998) *Chem Commun* 2345
- Wood A, Giersig M, Mulvaney P (2001) *J Phys Chem B* 105:8810
- Subramanian V, Wolf EE, Kamat PV (2004) *J Am Chem Soc* 126:4943
- Subramanian V, Wolf EE, Kamat PV (2003) *J Phys Chem B* 107:7479
- Zhang LZ, Yu JC, Yip HY, Li Q, Kwong KW, Xu AW, Wong PK (2003) *Langmuir* 19:10372
- Rajh T, Chen LX, Lukas K, Liu T, Thurnauer MC, Tiede DM (2002) *J Phys Chem B* 106:10543
- Book of ASTM standards (1969) American Society for Testing and Materials, part 25, Philadelphia, p 102
- Book of ASTM standards (1969) American Society for Testing and Materials, part 25, Philadelphia, p 579
- Fan SQ, Li CJ, Li CX, Liu GJ, Yang GJ, Zhang LZ (2006) p 1703
- Claus P, Hofmeister H (1999) *J Phys Chem B* 103:2766
- Rajh T, Nedeljkovic JM, Chen LX, Poluektov O, Thurnauer MC (1999) *J Phys Chem B* 103:3515
- Yu JC, Tang HY, Yu JG, Chan HC, Zhang LZ, Xie YD, Wang H, Wong SP (2002) *J Photochem Photobiol A* 153:211
- Xu CJ, Xu KM, Gu HW, Zheng RK, Liu H, Zhang XX, Guo ZH, Xu B (2004) *J Am Chem Soc* 126:9938